

## Recent multi-wavelength studies of gamma-ray binary hosting Be star

---

**Jumpei Takata\***

*School of Physics, Huazong University of Science and Technology*

*E-mail: takata@hust.edu.cn*

In the proceeding, first we will summarize results of our recent observations for gamma-ray binaries hosting Be star, HESS J0632+057 and PSR J2032+4127/MT91 213. For HESS J0632+057, Moritani et al. proposes a new binary parameter, which is smaller system size and smaller eccentricity comparing to the previous results. PSR J2032+4127 is the new gamma-ray binary confirmed by the VERITAS and MAGIC collaborations. We report the evolution of the optical/UV/X-ray light curves as the pulsar approaches to 2017/2018 periastron passage. We discuss the temporal variability of the emission from the gamma-ray binary with the pulsar binary model, and apply the discussion for the X-ray light curve of PSR J2032+4127/MT91 213 to investigate the evolution of the magnetization of the pulsar wind.

*7th Fermi Symposium 2017*

*15-20 October 2017*

*Garmisch-Partenkirchen, Germany*

---

\*Speaker.

Parameter	Casares et al. 2012	Moritani et al. 2017	
$P_o$ [day]	321	308	313
$T_0$ [day]	2455167.907	$2455076 \pm 10$	$2455065 \pm 11$
$\phi^a$	0.967	0.709	0.663
$e$	$0.83 \pm 0.08$	$0.62 \pm 0.16$	$0.64 \pm 0.29$
$\omega$ [deg]	$129 \pm 17$	$249 \pm 26$	$271 \pm 29$
$K_1$ [km s $^{-1}$ ]	$22.0 \pm 5.7$	$6 \pm 1$	$5 \pm 2$
$\gamma$ [km s $^{-1}$ ]	$48.3 \pm 8.9$	$36.9 \pm 0.8$	$36.7 \pm 0.9$
$a_1 \sin i$ [AU]	$0.362 \pm 0.261$	$0.136 \pm 0.029$	$0.120 \pm 0.029$
$f$ [ $M_{\text{sun}}$ ]	$0.06^{+0.15}_{-0.05}$	$0.0035 \pm 0.0022$	$0.0024 \pm 0.0017$

a: The phase at periastron

**Table 1:** Proposed orbital parameter of HESS J0632+057. Adapted from Moritani et al. 2017.

## 1. Introduction

The gamma-ray binary is a rare class of the binary system emitting GeV/TeV gamma-rays, and comprises a compact object (young neutron star/pulsar or black hole) and a high mass OB star (Dubus 2013). Their radiation spectra have a peak in  $\nu F_\nu$  around MeV/GeV bands, and extends up to  $\sim$  TeV. Seven gamma-ray binaries have been detected so far, namely PSR B1259-63/LS2883 (Aharonian et al. 2005), LS 5039 (Aharonian et al. 2005), LS I+61 $^\circ$ 303 (Albert et al. 2006), 1FGL J1018.6-5856 (Ackermann et al. 2012), HESS J0632+057 (Hinton et al. 2009), LMC P3 (Corbet et al. 2016) and PSR J2032+4127/MT91 213 (The VERITAS and MAGIC collaborations, ATel 10851). All gamma-ray binaries can be seen by X-ray, GeV and TeV telescopes.

Same as the high-mass X-ray binaries, the gamma-ray binaries are divided into two types, depending on the massive companion star, that is, Be-type star or O/B super giant. The gamma-ray binary hosting Be star (PSRs B1259-63, J2032+4127, LS I+63 $^\circ$ 303 and HESS J0632+057) shows an orbital period ( $P_b$ ) of months to years and an elliptical orbit with an eccentricity  $e > 0.5$ , while it hosting O/B star (LS 5039, 1FGL J1018.6-5856, LMC P3) has  $P_b < 30$ days and  $e < 0.5$ .

In this proceeding, first we will summarize results of our recent observations for gamma-ray binaries hosting Be star, HESS J0632+057 and PSR J2032+4127/MT91 213. Then, we will discuss the mechanism of the temporal variability of the emission with the pulsar binary model. Finally, we will interpret the rapid increase in the X-ray emission from PSR J2032+4127/MT91 213 with the inter-binary shock due to an interaction between the pulsar and stellar winds.

## 2. Orbital parameter of HESS J0632+057

HESS J0632+057 was discovered as a TeV gamma-ray source (Aharonian et al. 2007), and the follow-up observations found the periodic emissions in X-ray and TeV bands (Hinton et al. 2009; Aliu et al. 2014). In this binary system, the compact object is orbiting around the Be star with  $P_o \sim 315$ days and  $e \sim 0.83$  (Casares et al. 2012). The GeV emission was detected by a deep search in nearly nine years of the Fermi-LAT data (Li et al. 2017). Intriguing emission property of this system is X-ray/TeV flares occurred before and after apastron. The X-ray/TeV flares would

indicate the pulsar/Be disk interaction, provided the compact object is pulsar. However, the orbit parameters indicate that the compact object around the apastron is  $100R_{Be}$  far from the Be star, where  $R_{Be}$  is the radius of the Be star. For such a long distance, it would be difficult to explain the X-ray/TeV flares, because the Be disk density will be too low to stop the pulsar wind.

New optical observations were carried out using the 188cm telescopes at Okayama Astrophysical Observatory (4200-7400Å wavelength range), and monitored the source for four years to cover the entire orbital phase (Moritani et al. 2015, 2017). The radial velocity has been measured for H $\alpha$  emission line, and is interpreted by the binary model. New orbital parameters, comparing with Casares et al. (2012), are summarized in Table 1. We hold the data with the orbital period  $P_o = 308$  days, which provides the best fit of the optical data, and  $P_o = 313$  days predicted by the X-ray observation. The obtained parameters for two orbital periods are not different much each other, but show a large difference from the parameters in the previous study.

New orbital parameters show that system size is  $a_1 \sin i \sim 0.12$  AU, which is one third of the system size of Casares et al. (2012). The orbit of the compact object is more circular with the eccentricity  $e \sim 0.64$  than the previous case ( $e \sim 0.83$ ). This new orbital parameter also changes the position of the X-ray flares; the primary X-ray flare is occurred before the periastron and the secondary flare is located after the periastron. This position of the X-ray flares will be more consistent with the picture that the emission enhancements occur when the compact object passes the dense Be disk region. The mass function implies that mass of the compact object is less than  $2.5M_{\odot}$  unless the face on binary system, suggesting that the compact object is a pulsar.

### 3. Long orbit gamma-ray binary: PSR J2032+4127/MT91 213

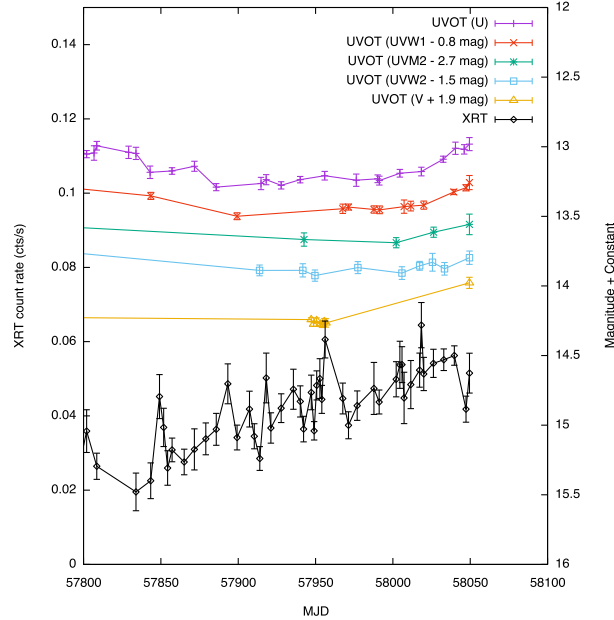


**Figure 1:** Orbital evolution of the X-ray and UV emission from PSR J2032+4127/MT91 213 in 2017, but before periastron.

PSR J2032+4127 is a radio-loud gamma-ray emitting pulsar discovered by the Fermi-LAT, and it is a young pulsar with a spin period  $P = 143\text{ms}$  and spin-down power  $L_{sd} \sim 1.7 \times 10^{35}\text{erg s}^{-1}$ . This pulsar had been regarded as isolated pulsar, but later identified as a binary system with further radio observations (Lyne et al. 2015). In this system, the pulsar is orbiting around the Be star with an orbital period of  $P_o \sim 50$  years (Ho et al. 2017). Recent periastron passage of the pulsar is occurred at later 2017/early 2018.

A TeV enhancement in September 2017 was detected by VERITAS and MAGIC collaboration (ATel 10810) and the observation confirmed that this binary system is indeed the gamma-ray binary. This binary system was observed as a faint X-ray source with  $F_X \sim 10^{-14}\text{erg cm}^{-2}\text{s}^{-1}$  before 2013. However the observed X-ray flux was  $\sim 10$  times brighter in 2015 and rapidly increases at the pulsar approaching to the periastron (Figure 1). All these observations strongly indicates an interaction between the pulsar and stellar winds (Takata et al. 2017; Li et al. 2017)). The brightness of UV also increases in 2016-2017 as the pulsar approaches to the periastron. This may be due to the shock heating of the stellar wind. The Be star in this gamma-ray binary system was observed by the 2-m Liverpool Telescope to monitor the evolution of the equivalent width (EW) of the  $H\alpha$  emissions. The EW was significantly decreases as  $-13.4\text{\AA}$ ,  $-12.4\text{\AA}$ , and  $-9.6\text{\AA}$  on 2017 July 25, August 14, and October 06, respectively, indicating that the Be disk is influenced by the pulsar wind. The monitoring of the periastron passage in 201/2018 by the multi-wavelength bands will provide us a lot of information on not only the pulsar wind physics, but also the Be disk, such as the density and the recovery from the disruption by the pulsar wind.

#### 4. Temporal variability

The gamma-ray binaries exhibit large temporal variations in its emission and spectrum along the orbital phase. We can also see the variation with a time scale shorter (Figure 1) or longer than the orbital period. The different gamma-ray binaries have a different property in the temporal variation. Moreover, the temporal variation is very stable (even for short time scale variation) every orbit, which may be more easily explained by the pulsar binary scenario than the black hole binary scenario. The temporal variability of the gamma-ray binary is not straightforward but it will contain various information on the physics of the gamma-ray binaries. With the pulsar binary model, seven mechanisms, at lease, can produce the temporal variability.

##### 4.1 Orbital motion

The orbit of the gamma-ray binary is elongated, and the separation between the compact object and the companion star can significantly vary along the orbit. With the pulsar binary model, the intra-binary shock due to the interaction between the pulsar and stellar winds is located at  $r_s \sim [\eta^{1/2}/(1 + \eta^{1/2})]a$  from the pulsar, where  $a$  is the separation and  $\eta \equiv L_{sd}/(\dot{M}_w v_w c)$  is the momentum ratio of the two wind and  $a$  is the separation between two stars. For example, the location of the intra-binary shock of the PSR B1259-63/LS 2883 system is estimated as  $r_s \sim 0.5\text{AU}$  at the periastron and  $r_s \sim 5\text{AU}$  at the apastron (Takata & Taam 2009). This large variation can make an adiabatic and a radiation cooling time scales of the shocked electrons/positrons depending on the orbital phase. The variation cooling time scale along the orbital phase can produce the temporal variation of the observed emission (e.g. Khangulyan et al. 2007). A large variation of the shock

distance from the pulsar could also produce a variation in the magnetization of the pulsar wind at the shock with the orbital phase (Takata & Taam 2009) and results in the temporal variability of the observed emissions.

#### 4.2 Pulsar/Be disk interaction

PSR B1259-63/LS3883 has been observed with the X-ray and TeV emission that increases when the pulsar passes the dense Be disk region. There is also indication of the pulsar/Be disk interaction at the X-ray/TeV flare of HESS J0632+057; the column density in the bright stage is higher than in the faint stage (Moritani et al. 2017). How to interact between the pulsar and Be wind/disk has been investigated by the SPH simulation (Takata et al. 2012). For the pulsar wind/stellar wind injection stage, a large fraction of the pulsar wind can escape from the system without the formation of the shock. For the pulsar wind/Be disk interaction stage, on the other hand, the most of the pulsar wind can be stopped by the Be disk matter and is injected into the shock. Other model is called *flip-flop* scenario, in which the emission during the pulsar's disk passage is produced under the propeller effect of the accretion matter on the pulsar magnetosphere (Papitto et al. 20012). It is also discussed a transient disk around the pulsar when the pulsar passes the Be disk (Takata et al. 2017)

With a simple analytics for the pulsar/Be disk interaction, the radius of the shock from the pulsar is estimated as  $r_s = [L_{sd}/(2\pi\rho_d v_r^2 c)]^{1/2}$ , where  $v_r$  is the relative velocity between the pulsar and the disk rotation, and it is typically  $v_r \sim 5 \times 10^7 \text{ cm s}^{-1}$ . The decretion disk model predicts disk mass density and the scale height of  $\rho_d(R) \propto \rho_0 (R_{Be}/R)^n$  and  $H(R) = H_0 (R/R_{Be})^\beta$ , respectively, where  $n \sim 3 - 3.5$  and  $\beta \sim 1 - 1.5$ . The density and the scale height at the stellar surface is of the order of  $\rho_0 \sim 10^{-11} - 10^{-9} \text{ g cm}^{-3}$  and  $H_0 \sim 0.01 R_{Be}$ , respectively (Okazaki et al. 2011). A pulsar/Be disk interaction will cause a cavity in the pulsar wind around the pulsar and will affect the observed emission, provided that  $r_s/H(a) < 1$ . Takata et al. (2017) applied this scenario to PSR J2032+4127/MT91 213 and found that a large base density  $\rho_0 \sim 10^{-9} \text{ g cm}^{-3}$  is required to confine most of the pulsar wind by the disk matter.

#### 4.3 Doppler boosting

The relativistic hydrodynamic calculation show that the rapid adiabatic expansion can accelerate the shocked pulsar wind to the relativistic speed (Bogovalov et al. 2012). Since the shock-cone wraps the pulsar, the Doppler boosting enhances the emissions around the inferior conjunction of the pulsar orbit, and suppresses the emissions around the superior conjunction. This effect will be more important to explain the orbital modulation for compact binary system, such as LS 5030 (Dubus 2010) and 1FGL J1018.6 (An and Romani 2017).

#### 4.4 An isotropic inverse-Compton scattering

The inverse-Compton process between the pulsar wind and stellar photon field will produce GeV/TeV emission from the gamma-ray binary. The gamma-rays observed at the different orbital phase are produced by the different collision angle. Around the inferior conjunction, since the observed photon is produced by tail-on collision, the emissivity is suppressed, while around the superior conjunction, the observed emissivity is enhanced by the head-on collision process (Dubus et al. 2008).

#### 4.5 Pair-creation cascade

If the separation between the pulsar and the companion star is close enough, the TeV emitted toward O/B star will be totally absorbed. The secondary electron and positron pairs created around the B star will also emit the non-thermal photons via the synchrotron and the inverse-Compton scattering process, and may initiate a further pair-creation cascade. If these pairs are isotropize, they will emit the photons propagating toward the observer, even though the primary TeV photons do not do this (Bednarek 1997; Cerutti et al. 2010).

#### 4.6 Clumpy stellar wind/anisotropic wind

It has been discussed that a radiatively non-stationary acceleration process produces a small-scale density inhomogeneity (clumping) of the stellar wind from the high-mass star (Runacres & Owocki 2002). The size of the clumping linearly expands from  $\sim 0.01R_{Be}$  with the radial distance, and a large structure of the clumps can be formed in the stellar wind. Although the clumps fill only a small fraction of the volume of the wind region, they carry most of mass ejected from the star, and have a mass density larger than the average density of the wind. The observed short time scale variability ( $\sim 1$ day) of the gamma-ray will be as a consequence of the pulsar wind/clumpy wind interaction (Bosch- Ramon 2013).

Beside a small scale structure of the stellar wind, there is a large structure of the anisotropy. The OB star will be driven by the radiation pressure, and the rapidly rotating main-sequence star (such that the angular velocity of the spinning is close to its Keplerian angular velocity) produces a stellar wind enhanced in the polar region, which results in the distribution of the stellar wind momentum. Since the shock distance from the pulsar and hence the emissivity of the shock emission depend on the momentum ratio of the two winds, the anisotropic stellar wind can produce the orbital modulation of the emission (Petropoulou et al. 2017).

#### 4.7 Evolution of the Be disk

The gamma-ray binary LS I +61°303 with  $P_o \sim 26$ days shows a long-term  $\sim 1667$ days periodic signal in the emission from all the wavelengths (e.g. Ackermann et al. 2013). How the superorbital variations are produced in LS I 61°303 is still under debate, it will be related to the evolution of the Be disk.

### 5. Pulsar wind of PSR J2032+4127/MT91 213

As we described in section 3, the observed X-ray flux of PSR J2032+4127/MT91 213 increased by a factor of ten during 2013-2015. However, the separation of the pulsar and Be star changed by only factor of two during 2013-2015, and it is therefore expected that the shock distance from the pulsar changed by a factor of two as well. With a pure synchrotron emission model, the radiation power is proportional to  $L_{syn} \propto r_s B^2(r_s) \propto r_s^{-1}$ , which cannot explain the observed increase of the X-ray emission. Effect of the interaction of the pulsar and Be disk before 2017 will not be important process, because the pulsar is far away from the Be star. The Doppler boosting is one possible scenario for the rapid increase in the observed X-ray flux. Before 2017, however, since the angle between the direction of the shock cone and the Earth viewing angle did not change much, it



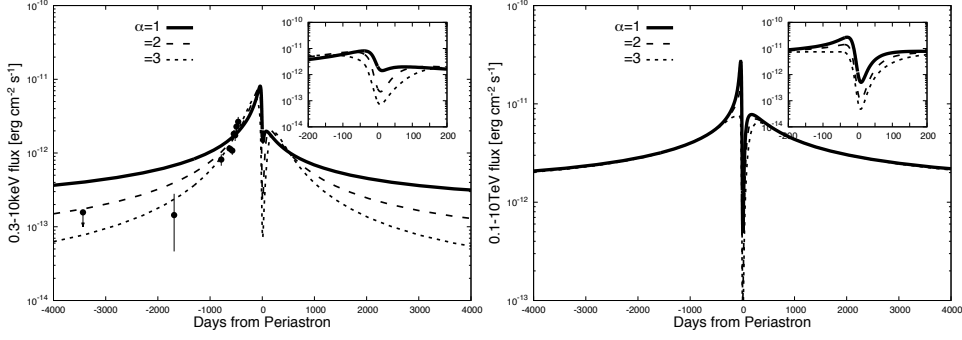


**Figure 2:** Adopted from Takata et al. (2017). The calculated orbital modulation in X-ray (left) and the TeV energy (right) bands. The solid, dashed and dotted lines are results for  $\alpha = 1, 2$  and  $3$ , respectively in  $\sigma \propto r^{-\alpha}$ .

is difficult to reproduce the observed X-ray light curve with a reasonable parameters (Takata et al. 2017). Petropoulou et al. (2017) explains the X-ray light curve with anisotropic stellar wind.

We may discuss that the rapid increase in the X-ray emission attributes for a radial evolution of the magnetization of the pulsar wind. The magnetization parameter,  $\sigma$ , is defined by the ratio of the particle energy to the kinetic energy,  $\sigma = B^2 / (4\pi\Gamma_{PW}N_{PW}m_e c^2)$ . It has been discussed that an energy conversion from the magnetic energy to particle energy decreases the magnetization from  $\sigma \sim 10^3-5$  at the light cylinder of the pulsar to  $\sigma < 1$  at the shock located far from the pulsar. How the magnetization evolves with the distance is still unknown, but  $\sigma \propto 1/r$  is suggested by the acceleration model (Kirk & Mochol 2011).

The magnitude of the magnetization parameter at the shock affects to the synchrotron emissivity of the shock emission (Dubus 2006; Takata et al. 2017), because the magnitude of the magnetic field tends to increase as the magnetization increases, while the total particle energy decreases. The former tends to increase the observed X-ray emission, while the latter decreases it. These two effects compensate each other and therefore the total power of the synchrotron emission from the shocked pulsar wind becomes maximum at the magnetization parameter  $\sigma \sim 0.1$ .

We fit the observed X-ray light curve by assuming the radial dependency of the magnetization as  $\sigma \propto r^{-\alpha}$ , where  $\alpha$  is the model fitting parameter. A rapid increase in the X-ray emission during 2013-2015 implies the power law index of  $\alpha = 2 - 3$  (Figure 2), although the evolution is much faster than  $\alpha = 1$  predicted by the acceleration model of the pulsar wind (Kirk & Mochal 2011).

If the evolution of the magnetization follows  $\sigma \propto r^{-\alpha}$  with  $\alpha = 2 - 3$ , the model predicts that the magnitude of the magnetization parameter at the shock exceeds the unity and hence the emission from the shock rapidly decreases as the pulsar approaches to the periastron. Hence this model can be tested by the observations for the periastron passage. The model also predicts the increase in the TeV emission from the inverse-Compton scattering process before the periastron, which is consistent with the discovery of the TeV enhancement by the VERITAS and MAGIC collaboration. The current model predicts a sharp drop of the TeV flux at the periastron passage because of the magnetization parameter larger than unity and because of the photon-photon pair-creation process. Takata et al. (2017) estimated the GeV flux averaged over the periastron passage is of the order of  $10^{-11} \text{erg cm}^{-2} \text{s}^{-1}$ , which is one order of magnitude smaller than that of the GeV

pulsed emission from the magnetosphere. Hence no prominent change in the GeV flux would be observed during the periastron passage of this system.

In summary, our optical observation suggests new orbital parameter of HESS J0632+057, and X-ray/TeV flares are occurred before and after the periastron. which is contradict to the case in the previous parameter. PSR J2032+4127/MT91 213 is the new gamma-ray binary with  $P_o \sim 50$ years, and the pulsar passes the periastron in 2017/2018. The temporal variations of the emission from the gamma-ray binaries are very complex, but contain a lot of the information to study the physics the pulsar wind and stellar wind/disk.

## Acknowledgments

I thank to Dr Y. Moritani for useful discussion for the orbital parameter of HESS J0632+057 and Drs K.L. Li and A.K.H. Kong for analyzing Swift for PSR J2032+4127. I also thank to Prof. K.S. Cheng for useful discussion for the emission process of the gamma-ray binaries. This work is supported by NSFC grants of Chinese Government under 11573010, U1631103 and 11661161010.

## References

- [1] Ackermann, M. et al. *Associating Long-term  $\gamma$ -Ray Variability with the Superorbital Period of LS +61 303 Periodic Emission from the Gamma-Ray Binary 1FGL J1018.6-5856*, *ApJ Letter* (2013), **773**, 35
- [2] Ackermann, M. et al. *Periodic Emission from the Gamma-Ray Binary 1FGL J1018.6-5856*, *Science* (2012) , **335**, 189
- [3] Aharonian, F. et al. *Discovery of a point-like very-high-energy  $\gamma$ -ray source in Monoceros*, *A&A Letter* (2007) , **469**, 1
- [4] Aharonian, F. et al. *Discovery of Very High Energy Gamma Rays Associated with an X-ray Binary*, *Science* (2005) , **309**, 746
- [5] Aharonian, F. et al. *Discovery of the binary pulsar PSR B1259-63 in very-high-energy gamma rays around periastron with HESS*, *A&A* (2005) , **441**, 465
- [6] Albert, J. et al. *Variable Very-High-Energy Gamma-Ray Emission from the Microquasar LS I +61 303*, *Science* (2006), **312**, 1771
- [7] Aliu, E. et al. *Long-term TeV and X-Ray Observations of the Gamma-Ray Binary HESS J0632+057*, *ApJ* (2014), **780**, 168
- [8] An, H. & Romani, R. W. *Light Curve and SED Modeling of the Gamma-Ray Binary 1FGL J1018.6-5856: Constraints on the Orbital Geometry and Relativistic Flow*, *ApJ* (2017), **838**, 145
- [9] Bednarek, W. *Cascade initiated by VHE  $\gamma$ -rays in their radiation field of a close massive companion*, *A&A* (1997), **322**, 523
- [10] Bogovalov, S. V. et al. *Modelling the interaction between relativistic and non-relativistic winds in the binary system PSR B1259-63/SS2883- II. Impact of the magnetization and anisotropy of the pulsar wind*, *MNRAS* (2012) , **419**, 3426
- [11] Bosch-Ramon, V. *Clumpy stellar winds and high-energy emission in high-mass binaries hosting a young pulsar*, *A&A* (2013), **560**, 32



- [12] Casares, J. et al. *On the binary nature of the  $\gamma$ -ray sources AGL J2241+4454 (= MWC 656) and HESS J0632+057 (= MWC 148)*, *ApJ* (2012) , **421**, 1103
- [13] Cerutti, B et al. *Modeling the three-dimensional pair cascade in binaries. Application to LS 5039*, *A&A* (2010) , **519**, 81
- [14] Corbet, R.H.D. et al. *A Luminous Gamma-ray Binary in the Large Magellanic Cloud* , *ApJ* (2016) , **829**, 105
- [15] Dubus, G. *Gamma-ray binaries and related systems* , *A&ARv* (2013) , **21**, 64
- [16] Dubus, G.; Cerutti, B.; Henri, G. *Relativistic Doppler-boosted emission in gamma-ray binaries* , *A&A* (2013) , **516**, 18
- [17] Dubus, G.; Cerutti, B.; Henri, G. *The modulation of the gamma-ray emission from the binary LS 5039*, *A&A* (2008) , **477**, 691
- [18] Dubus, G. *Gamma-ray binaries: pulsars in disguise?*, *A&A* (2006) , **456**, 801
- [19] Hinton, J. A. et al. *HESS J0632+057: A New Gamma-Ray Binary?*, *ApJ Letter* (2009) , **690**, 101
- [20] Ho, W.C.G. et al. *Multiwavelength monitoring and X-ray brightening of Be X-ray binary PSR J2032+4127/MT91 213 on its approach to periastron*, *MNRAS* (2017) , **464**, 1211
- [21] Khangulyan, D.; Hnatic, S.; Aharonian, F.; Bogovalov, S. *TeV light curve of PSR B1259-63/SS2883*, *MNRAS* (2007) , **380**, 320
- [22] Kirk, J.G. & Mochol, I. *Charge-starved, Relativistic Jets and Blazar Variability*, *ApJ* (2011) , **729**, 104
- [23] Li, K.L. et al. *Swift, XMM-Newton, and NuSTAR Observations of PSR J2032+4127/MT91 213*, *ApJ Letter* (2017) , **843**, 85
- [24] Li, J. et al. *GeV Detection of HESS J0632+057*, *ApJ* (2017) , **846**, 169
- [25] Lyne, A.G. et al. *The binary nature of PSR J2032+4127*, *MNRAS* (2015) , **451**, 581
- [26] Moritani, Y. et al. *Orbital solution leading to an acceptable interpretation for the enigmatic gamma-ray binary HESS J0632+057*, *PASJ* (2017) , submitted
- [27] Moritani, Y. et al. *Probing the Nature of the TeV  $\gamma$ -Ray Binary HESS J0632+057 by Monitoring Be Disk Variability*, *ApJL* (2015) , **804**, 32
- [28] Okazaki, A. et al. *Hydrodynamic Interaction between the Be Star and the Pulsar in the TeV Binary PSR B1259-63/LS 2883*, *PASJ* (2011) , **63**, 893
- [29] Papitto, A.; Torres, D. F.; Rea, N. *Possible Changes of State and Relevant Timescales for a Neutron Star in LS I +61 303*, *ApJ* (2012), **756**, 188
- [30] Petropoulou, M. et al. *X-ray mapping of the stellar wind in the binary PSR J2032+4127/MT91 213*, *MNRASL* (2017), submitted
- [31] Runacres, M. C. & Owocki, S. P. *The outer evolution of instability-generated structure in radiatively driven stellar winds*, *A&A* (2002), **381**, 1015
- [32] Takata J. et al. *High-energy Emissions from the Pulsar/Be Binary System PSR J2032+4127/MT91 213*, *ApJ* (2017) , **836** 241
- [33] Takata, J. et al. *Modeling High-energy Light curves of the PSR B1259-63/LS 2883 Binary Based on 3D SPH Simulations*, *ApJ* (2012), **750**, 70
- [34] Takata, J. and Tamm, R.E. *Probing the Pulsar Wind in the  $\gamma$ -ray Binary System PSR B1259-63/SS 2883*, *ApJ* (2009), **702**, 100